

Accelerate Langevin Sampling with Birth-Death process and Exploration Component

Lezhi Tan* Jianfeng Lu†

May 10, 2023

Abstract

Sampling a probability distribution with known likelihood is a fundamental task in computational science and engineering. Aiming at multimodality, we propose a new sampling method that takes advantage of both birth-death process and exploration component. The main idea of this method is *look before you leap*. We keep two sets of samplers, one at warmer temperature and one at original temperature. The former one serves as pioneer in exploring new modes and passing useful information to the other, while the latter one samples the target distribution after receiving the information. We derive a mean-field limit and show how the exploration process determines sampling efficiency. Moreover, we prove exponential asymptotic convergence under mild assumption. Finally, we test on experiments from previous literature and compared our methodology to previous ones.

1 Introduction

Sampling high-dimensional distributions has widespread applications in fields such as machine learning, Bayesian inference, and molecular simulations. The most well-known approach is to construct a Markov chain with an invariant distribution agrees with the target distribution, such as Random-Walk Metropolis [1, 2], Unadjusted Langevin Algorithm and Metropolis Adjusted Langevin Algorithm [3, 4, 5, 6], Hamiltonian Monte Carlo [7, 8], and others. These methods have been proven to be highly efficient when the log-likelihood is convex, see for example [9, 10, 11, 12] and references therein. However, in reality, probability distributions are seldom logconcave and are often multimodal. Multimodality has long been a challenge in sampling, as it can impede samplers from jumping across low-probability regions to reach new high-probability regions. Under multimodality, most MCMC approaches based on localized proposing mechanisms fail to explore the entire state space efficiently, resulting in biased outputs [1, 2]. As a result, there is a great need for the development of efficient sampling methods for multimodal distributions.

For more efficient sampling algorithms, one hopes for faster convergence to the target distribution π , starting from some initial distribution. This objective can be broken down into three subtasks. The first is to explore the entire state space, which means finding all high-probability regions (or modes). The second is to make ρ , the sampling distribution, converge locally to π inside every high-probability region. The final task is to balance the weights of ρ in each high-probability region. The second task is equivalent to sampling a unimodal distribution, which is often log-smooth and log-concave. This is relatively easy, as there are many methods efficient for

*Peking University, tlz3339@stu.pku.edu.cn

†Duke University, jianfeng@math.duke.edu

log-concave sampling and their convergence has been well-studied for decades [9, 12, 13]. However, the first and the third ones are much more difficult when the target distribution exhibits multimodality.

Concerning the first task, tempering approach, in particular parallel tempering (PT) [14], is well-known for accelerating exploration. It involves constructing multiple parallel Markov chains that individually converge to tempered versions of the target distribution $\pi^\beta(x)$ for $\beta < 1$. At these warmer temperature levels, the multimodality of the target distribution is reduced, which allows the samplers to more easily jump across low-probability regions and explore the entire state space. On the other hand, while faster exploration at warmer levels may occur, it does not necessarily translate to faster exploration at the target level, because swapping between different temperature levels can be inefficient. While this can be overcome by increasing the number of temperature levels, running multiple levels of Markov chains simultaneously requires more memory and longer computation time.

In addition to the technique of swapping, there are other methods that leverage information from higher temperature Markov chains. One such approach is used in ALPS (Annealed Leap-Point Sampler), which was recently proposed by Tawn et al. [15]. It first uses optimization to locate modes at a higher temperature, and then directly integrates these modes into Metropolis-Hastings updates. This is in contrast to the traditional method of maintaining several parallel chains at descending temperatures. In our work, we adopt this approach and refer to it as the Exploration Component.

The third task involves adjusting the weights between different high probability regions, which requires transporting samplers from one region to another. One possible way is the birth-death process proposed in [16]. While the Langevin Dynamic combined with Birth-Death process (BDLS), as shown in [17], can achieve asymptotic exponential convergence rate independent of the spectral gap, the actual (pre-asymptotic) performance is limited by the exploration stage - where new modes of the distribution are discovered by the sampler. Only after all modes are discovered, BDLS becomes efficient in adjusting the samplers across them, and hence converges to the target distribution. Thus, while BDLS resolves the third task, it hinders upon the first task of exploration.

Taking into account the strengths and limitations of existing methods, we propose a combined algorithm that addresses the three tasks of exploration, convergence inside high probability regions, and balancing weights between them. Our new sampling algorithm, named BDEC, is based on Langevin sampling and incorporates the birth-death process (BD) and the exploration component (EC). To accomplish the first task, we use samplers at a warmer temperature to explore the state space, and employ EC to detect new modes and update the collection of modes. We then insert samplers around new modes via a Metropolis-Hastings step. Once the insertion is successfully done, we return to within-temperature moves at the original temperature using Langevin MCMC with BD. In this combination, Langevin ensures local convergence within each high probability region, while BD help achieve efficient balancing of weights, independent of the degree of multimodality.

Our contribution We propose a new sampling scheme BDEC, which combines BD and EC to accelerate Langevin dynamics. Through numerical experiments, we show that using BD and EC together dramatically accelerates the Langevin dynamics. Our algorithm has faster convergence rate than both BDLS and ALPS, and has less computational costs than ALPS.

For theoretical analysis, we consider our Markov Chain under mean-field limit and continuous time limit. We first analyze global convergence and explicitly show how it is restricted by

the exploration rate, i.e., how much of the state space has been explored. We then prove that the asymptotic convergence is exponential, which only depends on the spectral gap under mild assumptions. In particular, our analysis not only applies to the asymptotic regime where the state space is fully explored, but also taking into consideration the exploration phase. In comparison, most previous literature directly assume that the starting distribution has already covered the entire state space.

Related works Two important components in BDEC, the birth-death process and exploration component, are directly inspired by previous literature. The birth-death process allows for mixing between Markov chains, and is generated from non-local mass transport dynamics known as birth-death dynamics. [16] first combined the birth-death dynamics with Langevin dynamics, and its improved analysis was given by [17]. The birth-death dynamics has also been applied to accelerate training for neural networks in mean-field limit [18]. There is a large body of literature on sampling schemes with interacting particles, including BDLS [16], ensemble MCMC [19, 20] and SVGD [21, 22]. Although these methods can transport particles inside the explored area, their exploration speed is limited.

To accelerate the exploration process, we utilize an extra Markov chain at warmer temperature. The use of fact that exploration is faster at warmer temperature can date back to the distinguished Parallel Tempering [14, 23]. Recent improvements to PT include the optimal choice of temperature spacings [24], accelerating mixing between temperatures [25], using a weight-preserving version of tempered distributions [26], and a variant with infinite swapping limit [27]. Instead of swapping between multiple levels of Markov chains like PT, we only keep one extra Markov chain and extract useful information about modes, similar to the exploration component in ALPS [15]. We generate proposals according to Gaussian mixture approximations, and keep a reversible chain according to the distinguished Metropolis-Hastings mechanism [28]. Gaussian approximation based on mode location and hessian has been widely used in Bayesian inference, MCMC and stochastic process [29, 30]. Our use of Gaussian mixture approximation shares the same idea with mode jumping MCMC [31] that we both use optimization to locate modes and then construct approximations to target distribution based on Hessian at the modes. Mode jumping MCMC also allows for non-local movements, however, its exploration process is not augmented.

The exploration component was first proposed as a key part of ALPS algorithm in [15], followed by theoretical analysis in [32]. However, our use of the exploration component is not identical to ALPS. While [15] addressed the problem of low Metropolis-Hastings acceptance rates caused by significant skewness in the target distribution, they did so by using annealing [33, 34]. Specifically, they employed several annealed Markov chains at colder temperatures, performing Metropolis-Hastings only at the coldest temperature, and swapped samplers between different temperature levels to insert new modes into the target level. Inevitably, this strategy leads to large memory and computational costs, similar to PT. In contrast, we show in our work that annealing is not necessary for our approach. The use of the Birth-Death process means that even with relatively low MH acceptance rates, a single accepted proposal can result in immediate transportation of enough samplers to new modes.

2 The Algorithm

Before we present the algorithm, let us first collect the notations used.

Notations

- $\pi(x) \propto e^{-V(x)}$, the target probability density; $\pi_\beta(x) \propto e^{-\beta V(x)}$, the tempered version that shares the same modes with π , with $\beta = 1$ corresponds to the target distribution. Here and in the sequel, we will abuse notation of distribution with its density.
- $\beta_{\text{hot}} < 1$, the inverse temperature of the warmer level for exploration;
- m_t , the number of mode points discovered by time t ; when no confusion might occur, it will be also abbreviated as m ;
- $M^t := \{\mu_1, \dots, \mu_{m_t}\}$, the mode locations of π discovered by iteration t ;
- $S^t := \{\Sigma_1, \dots, \Sigma_{m_t}\}$, the collection of covariance matrix,

$$\Sigma_i = -[\nabla^2 \log(\pi(\mu_i))]^{-1}, \quad i = 1, \dots, m_t;$$

- $W^t = \{\hat{w}_1, \dots, \hat{w}_{m_t}\}$, the collection of weights of modes,

$$\hat{w}_j = \frac{\pi(\mu_j)|\Sigma_j|^{1/2}}{\sum_{k=1}^{m_t} \pi(\mu_k)|\Sigma_k|^{1/2}}, \quad j = 1, \dots, m_t \quad (1)$$

- $I^t = \{M^t, S^t, W^t\}$ the information of modes collected by iteration t . We also abbreviate these notations as $I = \{M, S, W\}$ when there is no confusion.
- $\hat{\rho}(\cdot; I)$, the Gaussian mixture approximation of π based on the information of modes I ,

$$\hat{\rho}(x; I) = \sum_{i=1}^m \hat{w}_i \mathcal{N}(x; \mu_i, \Sigma_i) \quad (2)$$

- $P(x; y, I)$, the corresponding transition probability from y to x in Metropolis-Hastings updates:

$$P(x; y, I) = \hat{\rho}(x; I)A(x, y) + \mathbf{1}\{x = y\}(1 - \int \hat{\rho}(s; I)A(x, y)ds)$$

where $A(x, y)$ denotes the acceptance rate of proposing x from y ,

$$A(x, y) = \min\left\{1, \frac{\hat{\rho}(y; I)\pi(x)}{\hat{\rho}(x; I)\pi(y)}\right\} \quad (3)$$

- $X^t := \{x_1^t, x_2^t, \dots, x_N^t\}$, $Y^t = \{y_1^t, y_2^t, \dots, y_{\hat{N}}^t\}$, the collections of particles at original temperature and the warmer temperature by iteration t , respectively, where $N(\hat{N})$ denotes the number of particles at target (tempered) level, usually, we have $N \geq \hat{N}$;
- $K(\cdot, \cdot)$, the kernel function; $\rho_t(\cdot)$, the kernalized density of X^t :

$$\rho_t(\cdot) = \frac{1}{N} \sum_{i=1}^N K(x_i^t, \cdot). \quad (4)$$

2.1 Algorithm outline

The BDEC algorithm utilizes two groups of samplers X, Y at two different temperature levels: At target level, set as $\beta = 1$, X samples the target probability distribution $\pi(x)$; at warmer level, $\beta_{hot} < 1$, Y samples the tempered version of probability distribution $\pi_{\beta}(x)$. Samplers Y explore the state space faster than X thanks to its higher temperature.

There are two kinds of moves: within-temperature moves and interaction between two levels. We use birth-death accelerated Langevin sampling (BDLS) [16] for within-temperature updates of X , and unadjusted Langevin algorithm for within-temperature updates of Y .

After every T within-temperature moves, the exploration component collects the information provided by Y and passes it to X , which is interpreted as interaction between two levels. First, the algorithm locates a bunch of modes by optimization on the potential surface starting at a subset of Y , aiming to find new modes (local minima). These modes will help the sampler X by proposal of new locations incorporating such modes together with a Metropolis-Hastings acceptance-rejection to ensure that X samples the correct distribution. Benefit by the exploration component, X is not limited by the exploration given by the Langevin dynamics at the original temperature.

The outline of the BDEC procedure is given in Algorithm 1, the details of its constituent parts are elaborated in the following subsections 2.2, 2.3 and 2.4. The exploration component is introduced in subsection 2.3, while the birth-death process is introduced in subsection 2.4.2.

2.2 Within-temperature Updates at Tempered Level

The first stage in each iteration is the within-temperature moves of Y . We hope Y to serve as a pioneer in exploration, which means, samplers in Y should not be trapped in one high-probability region as long as those in X . Meanwhile, we hope samplers in Y do not jump away from any new high-probability region too soon, but to stay until information of this new region is successfully passed to X . For these reasons, we set Y as samplers of the tempered distribution $\pi_{\beta_{hot}}$. β_{hot} is a parameter to be tuned. As Y do not need to accurately converge to $\pi_{\beta_{hot}}$, we simply choose unadjusted Langevin algorithm [3] for its update (see algorithm 2). One could also choose other MCMC approaches in the implementations.

Algorithm 2 Unadjusted Langevin algorithm (ULA)

Initialization: $V(x)$, the log-likelihood of target distribution $\pi(x)$; inverse temperature, β ; an initial set of particles $\{y_i^0\}_{i=1}^{\hat{N}}$; T the number of updates, Δt the time step.

- 1: **for** $t \leftarrow 1$ to T **do**
 - 2: **for** $i \leftarrow 1$ to \hat{N} **do**
 - 3: set $y_i^t = y_i^{t-1} - \Delta t \cdot \beta \nabla V(y_i^{t-1}) + \sqrt{2\Delta t} \epsilon_i$, where $\epsilon_i \sim N(0, 1)$
 - 4: **end for**
 - 5: **end for**
-

2.3 Exploration Component

The second stage in each iteration is to collect useful information based on current locations of $\{y_j\}_{j=1}^{\hat{N}}$. The most useful information related to a new high-probability region is its mode. To this end, we introduce the exploration component (EC), a mode finding procedure proposed in [15] as a component of ALPS algorithm. We adopt the same scheme as ALPS: after T steps of

Algorithm 1 Langevin Sampling with Birth-Death Process and Exploration Component

Initialization: Hotter temperature β_{hot} ; initial mode point information $I^0 := \{M^0, S^0, W^0\}$; initial particles at the target temperature and the warmer temperature, $X^0 = \{x_i^0\}_{i=1}^N$, $Y^0 = \{y_j^0\}_{j=1}^{\hat{N}}$; a Metropolized transition operator, $P(\cdot; x, I)$; J the number of total iterations, and T the number of within-temperature moves in each iteration.

```
1: procedure BDEC( $X^0, Y^0$ )
2:   for  $j \leftarrow 1$  to  $J$  do
3:      $m \leftarrow (J - 1)T$ 
4:     1.Within-temperature Updates at Tempered Level:
5:     for  $t \leftarrow 1$  to  $T$  do
6:       Update:  $Y^{t+m} \leftarrow \text{Langevin}(Y^{t+m-1}; \beta = \beta_{\text{hot}})$ 
7:     end for
8:     2.Exploration Component: (apply Algorithm 3)
9:
10:       $I^{jM}, \text{New} \leftarrow \text{ModeFinder}(Y^{jM}, I^{(j-1)M})$ 
11:
12:     3.Within-temperature Updates at Target Level:
13:     if  $\text{New} == \text{True}$  then
14:       for  $t \leftarrow 1$  to  $T$  do
15:         Update:  $X^{t+m-1/2} \leftarrow P(\cdot; X^{t+m-1}, I^j)$ 
16:         Adjust:  $X^{t+m} \leftarrow \text{BD}(X^{t+m-1/2}, \cdot)$ 
17:       end for
18:     else  $\text{New} == \text{False}$ 
19:       Apply BDLS Algorithm 4:
20:       for  $t \leftarrow 1$  to  $T$  do
21:         Update:  $X^{t+m-1/2} \leftarrow \text{Langevin}(X^{t+m-1}; \beta = 1)$ 
22:         Adjust:  $X^{t+m} \leftarrow \text{BD}(X^{t+m-1/2}, \cdot)$ 
23:       end for
24:     end if
25:   end for
26:   return  $X^{JT}$ 
27: end procedure
```

diffusion at tempered level, we apply EC for once to locate modes and then decide whether a new mode (or new modes) is found.

EC consists of two steps: first, it finds the nearest mode μ_j to y_j^t through local optimization initialized from the current location of y_j^t ; second, it determines whether μ_j is a new mode or it has already been contained in M^t . Because N could be large and it would be wasteful to run optimization for every particles, the y_j^t will only be a batch of particles uniformly chosen from Y^t . The batch size B is a given parameter. Empirically, $B = 0.01N$ is used.

In order to decide whether μ_j is a new mode, it is necessary to define a distance between modes. One approach is presented in [15]:

$$D(\mu_k, \mu_l) := d^{-1} \max \{ (\mu_k - \mu_l)^T \Sigma_k^{-1} (\mu_k - \mu_l), (\mu_k - \mu_l)^T \Sigma_l^{-1} (\mu_k - \mu_l) \} \quad (5)$$

where d is the dimension. A threshold thr should be given. If for all μ^* in M^t , $D(\mu_j, \mu^*) > thr$, then μ_j is considered a new mode. Empirically we let $thr = 1 + (2/d)^{1/2}$, as suggested by [15].

Algorithm 3 The exploration component

Initialization: Particles at hotter temperature $Y^t = \{y_j^t\}_{j=1}^N$, and information of modes $I^t := \{M^t, S^t, W^t\}$ discovered by iteration t ; a threshold thr , and a batch size B .

```

1: procedure MODEFINDER( $Y^t, I^t$ )
2:   New = False
3:    $\bar{Y} = \{y_{k_1}, y_{k_2}, \dots, y_{k_B}\}$ , where  $k_1, \dots, k_B$  are uniformly chosen from  $\{1, 2, \dots, N\}$ 
4:   for  $b \leftarrow 1$  to  $B$  do
5:     Run: Quasi-Newton optimization initialized from  $y_b$  to get  $\bar{\mu}_b \in \mathbb{R}^d$ .
6:     Compute:
           
$$\bar{\Sigma}_b := -(\nabla^2 \log \pi(\bar{\mu}_b))^{-1}$$

7:     for  $k \leftarrow 0$  to  $m_t$  do
8:       Compute:  $d_k := D(\mu_k, \bar{\mu}_b)$  ▷ where  $D(\cdot, \cdot)$  is defined in (5)
9:     end for
10:    if  $\min\{d_1, \dots, d_{m_t}\} > thr$  then
11:      New = True
12:      Update  $I^t$  by adding the new mode information:
           
$$(\mu_{m_t+1}, \Sigma_{m_t+1}, \hat{w}_{m_t+1}) := (\bar{\mu}_b, \bar{\Sigma}_b, \bar{w}_b) \quad (6)$$

13:    end if
14:  end for
15: end procedure
16: return  $I^t$ , New

```

2.4 Within-temperature Updates at Target Level

2.4.1 Proposing new modes

The third stage in each iteration is within-temperature updates of X . There are two cases according to the output of EC:

1. If a new mode is found by EC, then the information about new mode needs to be passed to X . We incorporate the information into Gaussian approximation $\hat{\rho}(\cdot; I^t)$, defined in (2). The Gaussian mixture will serve as proposal distribution in Metropolis-Hastings steps. Denote the

N proposals at step t as $z_1^t, z_2^t, \dots, z_N^t \stackrel{iid}{\sim} \hat{\rho}(\cdot; I^t)$, the Metropolis-Hastings acceptance probability for each sampler is computed as:

$$A_i^t = \min\left\{1, \frac{\hat{\rho}(z_i^t; I^t)\pi(x_i^t)}{\hat{\rho}(x_i^t; I^t)\pi(z_i^t)}\right\}, \quad \text{for } i = 1, 2, \dots, N. \quad (7)$$

Then we assign $x_i^{t+1} = z_i^t$ with probability A_i^t , or $x_i^{t+1} = x_i^t$ otherwise. Through the MH step, some of the samplers are transported to the area around new modes, so the new high-probability regions are now covered by $\text{supp}(\rho_{t+1})$. After that, we apply the Langevin algorithm with birth-death process (BDLS) for updates of X . From previous literature [16], we know that birth-death process can transport particles between separated high-probability regions. Therefore, a bunch of samplers that clustered around old modes will be transported to the new modes with little samplers around.

2. If no new mode is found, we skip the Metropolis-Hastings steps and only apply BDLS for updates of X , as follows.

2.4.2 Birth-Death Process Accelerated Langevin Sampling

BDLS consists of two parts: local updates based on the unadjusted Langevin algorithm, and a birth-death process, as described in detail in [16] and restated in Algorithm 4. We choose BDLS because it extends beyond the limitations of local moves. The birth-death process allows the sampler to transition between high probability areas without being hindered by energy barriers.

Algorithm 4 Birth-death Process Accelerated Langevin Sampling (BDLS)

Initialization: $V(x)$, the log-likelihood of target distribution $\pi(x)$; a set of initial particles $\{x_i^0\}_{i=1}^N$; the kernel function K ; T the number of updates, Δt the time step.

```

1: for  $t \leftarrow 1$  to  $T$  do
2:   Langevin:
3:   for  $i \leftarrow 1$  to  $N$  do
4:     set  $x_i^t = x_i^{t-1} - \Delta t \nabla V(x_i^{t-1}) + \sqrt{\Delta t} \epsilon_i$ , where  $\epsilon_i \sim N(0, 1)$ 
5:   end for
6:   Birth-Death process:
7:   for  $i \leftarrow 1$  to  $N$  do
8:     calculate  $r_i = \log\left(\frac{1}{N} \sum_{l=1}^N K(x_i^t - x_l^t)\right) + V(x_i^t)$ 
9:   end for
10:  set  $\bar{r} = \frac{1}{N} \sum_{l=1}^N r_l$ 
11:  for  $i \leftarrow 1$  to  $N$  do
12:    if  $\beta_i > \bar{\beta}$  then
13:      kill  $x_i^t$  with probability  $1 - e^{(\bar{r}-r_i)\Delta t}$ ;
14:      duplicate one uniformly chosen from other  $X^t$ ;
15:    else
16:      duplicate  $x_i^t$  with probability  $1 - e^{(r_i-\bar{r})\Delta t}$ ;
17:      kill one uniformly chosen from other  $X^t$ .
18:    end if
19:  end for
20: end for

```

One interesting aspect of the birth-death process is that it can be interpreted as interaction between N samplers. Therefore, BDLS, as well as pure birth-death process, can be viewed as an

ensemble Markov Chain Monte Carlo approach, similar to another method recently proposed by Lindsey et al. [20]. Here, we provide a brief comparison between the pure birth-death process [16] and the Ensemble MCMC approach in [20], which also explains the reason that we take BDLs for weight adjusting in our method.

The pure birth-death process is a time discretization of the birth-death dynamic given by (8), similar to the PDE of Ensemble MCMC approach proposed in [20], as shown in (9), where \mathcal{Q} is a proposal distribution of Metropolis-Hastings. In both cases, the dynamics involve a term that depends on the ratio of the current density ρ to the target density π , a term that accounts for the interaction between samplers.

$$\frac{d\rho}{dt} = -\left(\frac{\rho}{\pi} - z_\rho\right)\rho, z_\rho := \int \frac{\rho(x)}{\pi(x)}\rho(x)dx \quad (8)$$

$$\frac{d\rho}{dt} = -\frac{1}{Z_\rho}\left(\frac{\rho}{\pi} - Z_\rho\right)\mathcal{Q}\rho, Z_\rho := \int \frac{\rho(x)}{\pi(x)}\mathcal{Q}\rho(x)dx \quad (9)$$

In practice, the proposal \mathcal{Q} is chosen as a local random walk, for example, Gaussian diffusion. Whether there is a proposal \mathcal{Q} is not the main difference between the two schemes, as [20] assumes in its theoretical part that \mathcal{Q} would converge to Id in the asymptotic limit. Under the limit $\mathcal{Q} \rightarrow \text{Id}$, (9) becomes

$$\frac{d\rho}{dt} = -\frac{1}{z_\rho}\left(\frac{\rho}{\pi} - z_\rho\right)\rho, \quad (10)$$

which differs from (8) only in scale. The difference in scale, which is the main difference we are concerned about, reflects difference in implementation. Although both algorithms need to calculate the rate $r(x) = \frac{\rho(x)}{\pi(x)} - z_\rho$ for N samplers in each iteration, the Ensemble MCMC only adjust one particle, while the birth-death process adjust the whole pack. Accordingly, the birth-death process is more cost-effective.

3 Theoretical Analysis

3.1 Main results

For the theoretical property of BDEC, we choose to analyze the continuous time sampling dynamic instead of discrete-time Markov Chain, since the analysis of convergence of former is easier and cleaner than that of a discrete process. Here, we only focus on the dynamic of X^t while leaving Y^t in the background, since we are only concerned about how samplers at original temperature converge. Of course, one should keep in mind that the exploration of Y^t plays an important role affecting the convergence of X^t .

Let us first present the continuous-time sampling dynamics. Let ρ_t denote the density of samplers X^t at target level by time $t > 0$. Let Ω denote the support of π and Ω_t denote the support of ρ_t . We assume $\rho_t \ll \pi$ throughout the whole process, which means $\Omega_t \subseteq \Omega$. The distribution evolves according to:

$$\partial_t \rho_t = \nabla \cdot (\rho_t \nabla V + \nabla \rho_t) - \tau_1 \alpha_t \rho_t + \tau_2 \int_{\Omega} R(x, y) (\pi(x) \rho_t(y) - \pi(y) \rho_t(x)) dy. \quad (11)$$

The three terms on the right hand side correspond to the following:

- The first one $\nabla \cdot (\rho_t \nabla V + \nabla \rho_t)$ stands for Langevin dynamics.

- The second one $-\tau_1\alpha_t\rho_t$ stands for the Birth-Death process, with birth/death rate

$$\alpha_t = \frac{\rho_t}{\pi} - \int_{\Omega_t} \frac{\rho_t^2}{\pi} dx.$$

The integral is subtracted in order to keep the normalization of density $\int_{\Omega_t} \rho_t dx = 1$.

- The third one stands for the Metropolis-Hastings step after new modes are found (see case 1 in section 2.4). We will use the shorthand notation $\hat{\rho}_t(x)$ for the proposal density $\hat{\rho}(x; I_t)$ (defined in (2)). The term $R(x, y)$ is then given by the MH acceptance rate $A(x, y)$ (defined in (3)) multiplying with $\hat{\rho}_t(x)/\pi(x)$:

$$R(x, y) = \min\left\{\frac{\hat{\rho}_t(x)}{\pi(x)}, \frac{\hat{\rho}_t(y)}{\pi(y)}\right\}.$$

One need to remember that, samplers at target level stay still during the mode finding process EC (see 2.3), but only do Metropolis-Hastings update afterwards. So throughout this section, we call this part of update ‘MH step’ instead of ‘EC’.

In (11), τ_1, τ_2 are parameters that determine the frequency (relative to the Langevin update) of Birth-Death step and Metropolis-Hastings step. In our implementation, $\tau_1 = 1$, as a Langevin update is always followed by a birth-death adjustment. In the implementation, the value of τ_2 depends on the frequency a new mode is discovered, and becomes 0 once all modes are found. However, for simplicity of the analysis, we can also assume $\tau_2 = 1$, which means, one step of MH update is carried out in each iteration. We first restrict to the case that τ_1, τ_2 are strictly positive in our main result (Theorem 1), and then we will discuss the case $\tau_2 = 0$ in Remark 1.4.

Let us define $g_t = \rho_t/\pi$, the density of the sampler with respect to the target. From (11) we get:

$$\partial_t g_t = -\nabla V \cdot \nabla g_t + \Delta g_t - \tau_1(g_t - \bar{g}_t)g_t + \tau_2 \int_{\Omega} \min(\hat{g}_t(x), \hat{g}_t(y))(g_t(y) - g_t(x))\pi(y)dy, \quad (12)$$

where $\bar{g}_t = \int_{\Omega} g_t^2 \pi dx$ and $\hat{g}_t = \hat{\rho}_t/\pi$. Based on this, we can analyze the convergence rate of ρ_t in the sense of χ^2 -divergence

$$D_t = \int_{\Omega} \frac{\rho_t^2}{\pi} dx - 1 = \int_{\Omega_t} \frac{\rho_t^2}{\pi} dx - 1 = \int_{\Omega_t} g_t^2 \pi dx - 1, \quad (13)$$

which would converge to 0 when $\rho_t \rightarrow \pi$, i.e., $g_t \rightarrow 1$.

Before presenting the result, we introduce a variable to quantify ‘exploration rate’:

$$Z_t := \int_{\Omega_t} \pi(x) dx \quad (14)$$

where $\Omega_t := \text{supp}(\rho_t)$ is the area X^t has explored. Based on assumption $\Omega_t \subseteq \Omega$ for all t , it is clear that $Z_t \in [0, 1]$. Along our sampling process, Ω_t is expanding, so Z_t is non-decreasing. Note that the χ^2 -divergence D_t is always larger than $\frac{1}{Z_t} - 1$,

$$(D_t + 1) \cdot Z_t = \int_{\Omega_t} \frac{\rho_t^2(x)}{\pi(x)} dx \cdot \int_{\Omega_t} \pi(x) dx \geq \left[\int_{\Omega_t} \rho_t(x) dx\right]^2 = 1 \quad (15)$$

which means, global convergence is always controlled by the exploration rate. Only when the whole state space has been fully explored ($Z_t = 1$), it would be possible for D_t to reach 0.

Our main theorem focuses on how ‘exploration rate’ plays a decisive role in the sampling process. The key assumption (16) will be discussed in section 3.3.

Theorem 1. Let ρ_t solve (11) for $t \geq 0, \tau_1, \tau_2 > 0$ and Z_t defined in (14). For any fixed $t_0 \geq 0$, suppose for some $c \in (0, 1)$ and any $t \geq t_0$,

$$\inf_{x \in \Omega} \frac{\hat{\rho}_t(x)}{\pi(x)} \geq c \quad (16)$$

holds, then

$$D_t + 1 - \frac{1}{Z_{t_0}} \leq \left(D_{t_0} + 1 - \frac{1}{Z_{t_0}} \right) \exp\{-2\kappa_1(t - t_0) - \kappa_2 e^{-c\tau_2(t-t_0)} + \kappa_2\} \quad (17)$$

holds for any $t \geq t_0$, where $\kappa_1 = 2\tau_1 + 2c\tau_2$, $\kappa_2 = \frac{2\tau_1(1-G_{t_0})}{\tau_2 c}$, and G_0 is defined in (21).

Remark 1.1. From (15), we know that RHS is always positive. Meanwhile, notice that it is $1/Z_{t_0}$ instead of $1/Z_t$ in LHS, so LHS is possible to be negative for large t .

Remark 1.2. One should also notice that the lower bound c in (16) varies according to t_0 . We will give an explicit estimation for c in subsection 3.3. Intuitively, larger the number of modes been discovered, larger the c would be. This is where Y^t comes into play. The exploration of Y^t directly decide how many of the modes have already been collected. Therefore, if exploration of Y^t is successful, c would be large for small t_0 , which means, the decay of D_t would be faster.

The theorem establishes local convergence of our sampling scheme. Here, ‘local’ refers to the limited region we have already explored compared to the whole state space. If unfortunately, the samplers are stuck inside Ω_{t_0} after time t_0 , then the best we can hope for is convergence to π restricted on Ω_{t_0} ($D_t \rightarrow 1 - 1/Z_{t_0}$) instead of π . On the other hand, the local convergence is exponential and independent of the energy barrier. This matches our analysis in section 1: the exploration of new modes is the decisive factor in overcoming multimodality.

A direct implication from Theorem 1 is that the asymptotic convergence is also exponential. Here, ‘asymptotic’ refers to the state after the whole state space has been completely explored, that is, $Z_t = 1$ for all $t \geq t_0$. Recall that Z_t is non-decreasing, so we only need $Z_{t_0} = 1$ for some $t_0 \geq 0$.

Corollary 1. Let ρ_t solve (11) for $t \geq 0, \tau_1, \tau_2 > 0$ and Z_t defined in (14). Suppose there exists $t_0 \geq 0$, such that

$$\Omega_{t_0} = \Omega \quad (18)$$

and (16) holds for any $t \geq t_0$. Then for any $t \geq t_0$,

$$D_t \leq D_{t_0} \exp\{-\kappa_1(t - t_0) - \kappa_2 e^{-c\tau_2(t-t_0)} + \kappa_2\}, \quad (19)$$

where $\kappa_1 = 2\tau_1 + 2c\tau_2$, $\kappa_2 = \frac{2\tau_1(1-G_{t_0})}{\tau_2 c}$, and G_{t_0} is defined in (21).

This corollary implies that, once the state space has been fully explored, the sampling density ρ_t will converge exponentially to π . It is worth noticing that, our dynamic (11) is exactly BDLS [16] if we set $\tau_1 = 1, \tau_2 = 0$. In our implementation, $\tau_1 = 1$, so the exponent of convergence rate κ_1 is at least 2, which means that our asymptotic convergence rate is no less than BDLS and is strictly larger when $\tau_2 > 0$.

Besides, our assumption is weaker on ρ_t . Instead of assuming a positive lower bound of $\rho_{t_0}(x)/\pi(x)$ (see Theorem 2.3 in [17]), our asymptotic analysis only require ρ_{t_0} to share the same support with π (18). However, we do need assumptions on the proposal $\hat{\rho}_t$. This point is further explained in Remark 1.3.

More importantly, in our dynamic, it takes less time for (18) to be satisfied. If (16) holds, then from (11) we know,

$$\partial_t \rho_t(x) = \tau_2 \int_{\Omega} R(x, y) \pi(x) \rho_t(y) dy > \tau_2 c \int_{\Omega} \pi(x) \rho_t(y) dy > 0$$

for all $x \in \Omega - \Omega_t$. This means, as long as the whole state space is explored at the tempered level and the proposal behaves well in the sense of (16), then our support Ω_t at target level will instantly expand to Ω . As comparison, in BDLS, the expansion of support is totally decided by the diffusion of Langevin dynamics at original temperature, which is much slower, thus it takes longer time to reach the condition $\Omega_t = \Omega$. This comparison again stresses the fact that performance of sampling algorithms highly relies on exploration process.

3.2 Proof of the theorem

Proof. Taking the derivative of the χ^2 divergence, we have

$$\begin{aligned} \frac{dD_t}{dt} &= 2 \int_{\Omega} g_t(x) \partial_t g_t(x) \pi(x) dx = 2 \int_{\Omega_t} g_t(x) \partial_t g_t(x) \pi(x) dx \\ &= 2 \int_{\Omega_t} g_t(x) \nabla \cdot (\pi(x) \nabla g_t(x)) dx - 2\tau_1 \int_{\Omega_t} (g_t - \bar{g}_t) g_t^2 \pi dx \\ &\quad + 2\tau_2 \int_{\Omega_t} \int_{\Omega} \min(\hat{g}_t(x), \hat{g}_t(y)) (g_t(y) - g_t(x)) g_t(x) \pi(x) \pi(y) dy dx \\ &= -2 \int_{\Omega_t} \pi (\nabla g_t)^2 dx - 2\tau_1 \int_{\Omega_t} (g_t - \bar{g}_t) g_t^2 \pi dx \\ &\quad - 2\tau_2 \int_{\Omega_t} \int_{\Omega} \min(\hat{g}_t(x), \hat{g}_t(y)) (g_t(y) - g_t(x)) g_t(x) \pi(x) \pi(y) dy dx \end{aligned} \quad (20)$$

The last equality is generated by using Gauss-Green formula $\int_{\Omega_t} \nabla \cdot (\pi g_t \nabla g_t) dx = \int_{\partial \Omega_t} \pi g_t \nabla g_t dt$. Notice that $g_t(x)|_{\partial \Omega_t} = 0$, so

$$\int_{\Omega_t} g_t(x) \nabla \cdot (\pi(x) \nabla g_t(x)) dx + \int_{\Omega_t} \pi (\nabla g_t)^2 dx = 0.$$

First we introduce two useful variable:

$$G_t = \inf_{\Omega_t(x)} \frac{\rho_t(x)}{\pi(x)}, \quad \hat{G}_t = \inf_{\Omega(x)} \frac{\hat{\rho}_t(x)}{\pi(x)} \quad (21)$$

Note that their domains of infimum are different.

Then we upper bound the right hand side of (20):

- The first term $-2 \int_{\Omega_t} \pi (\nabla g_t)^2 dx \leq 0$.
- The second term $-2\tau_1 \int_{\Omega_t} (g_t - \bar{g}_t) g_t^2 \pi dx = -2\tau_1 \int_{\Omega_t} (g_t - \bar{g}_t)^2 g_t \pi dx$. By Cauchy-Schwarz,

$$\int_{\Omega_t} (g_t - \bar{g}_t)^2 g_t \pi dx \int_{\Omega_t} \frac{(\rho_t - \pi/Z_t)^2}{\rho_t} dx \geq \left[\int_{\Omega_t} (g_t - \bar{g}_t) (\rho_t - \pi/Z_t) dx \right]^2$$

Notice that

$$\int_{\Omega_t} (g_t - \bar{g}_t) (\rho_t - \pi/Z_t) dx = -\frac{1}{Z_t} \int_{\Omega_t} (g_t - \bar{g}_t) \pi dx = D_t + 1 - \frac{1}{Z_t}$$

and

$$\int_{\Omega_t} \frac{(\rho_t - \pi/Z_t)^2}{\rho_t} dx \leq \frac{1}{G_t} \int_{\Omega_t} \frac{(\rho_t - \pi/Z_t)^2}{\pi} dx = \frac{1}{G_t} (D_t + 1 - \frac{1}{Z_t})$$

Then we obtain an upper bound for the second term

$$-2\tau_1 \int_{\Omega_t} (g_t - \bar{g}_t)^2 g_t \pi dx \leq -2\tau_1 G_t (D_t + 1 - \frac{1}{Z_t}) \quad (22)$$

• The third term

$$\begin{aligned} & -2\tau_2 \int_{\Omega_t} \int_{\Omega} \min(\hat{g}_t(x), \hat{g}_t(y)) (g_t(y) - g_t(x)) g_t(x) \pi(x) \pi(y) dy dx \\ &= -2\tau_2 \int_{\Omega^2} \min(\hat{g}_t(x), \hat{g}_t(y)) (g_t(y) - g_t(x)) g_t(x) \pi(x) \pi(y) dx dy \\ &= -\tau_2 \int_{\Omega^2} \min(\hat{g}_t(x), \hat{g}_t(y)) (g_t(y) - g_t(x))^2 \pi(x) \pi(y) dx dy \\ &\leq -\tau_2 \widehat{G}_t \int_{\Omega^2} (g_t(y) - g_t(x))^2 \pi(x) \pi(y) dx dy \\ &= -2\tau_2 \widehat{G}_t D_t \\ &\leq -2\tau_2 \widehat{G}_t (D_t + 1 - \frac{1}{Z_t}) \end{aligned} \quad (23)$$

In conclusion, we get

$$\frac{dD_t}{dt} \leq -[2\tau_1 G_t + 2\tau_2 \widehat{G}_t] (D_t + 1 - \frac{1}{Z_t})$$

Because Z_t is non-decreasing, we have for any fixed t_0 :

$$\begin{aligned} \frac{dD_t}{dt} &\leq -[2\tau_1 G_t + 2\tau_2 \widehat{G}_t] (D_t + 1 - \frac{1}{Z_{t_0}}), \forall t \geq t_0 \\ \implies D_t + 1 - \frac{1}{Z_{t_0}} &\leq (D_{t_0} + 1 - \frac{1}{Z_{t_0}}) \exp\{-\int_{t_0}^t (2\tau_1 G_s + 2\tau_2 \widehat{G}_s) ds\} \end{aligned} \quad (24)$$

After this, we intend to lower bound G_t . We can assume ρ_t and π are all twice continuously differentiable, then there exists $x_t \in \Omega$, that $\rho_t(x_t)/\pi(x_t) = G_t$, for every t . Hence we have $\nabla g_t(x_t) = 0, \Delta g_t(x_t) \geq 0$.

$$\begin{aligned} \frac{dG_t}{dt} &= \frac{dg_t(x_t)}{dt} = \nabla g_t(x_t) \cdot \frac{dx_t}{dt} + \partial_t g_t(x_t) \\ &= \Delta g_t(x_t) - \tau_1 (G_t - \bar{g}_t) G_t + \tau_2 \int_{\Omega} \min(\hat{g}_t(x_t), \hat{g}_t(y)) (g_t(y) - G_t) \pi(y) dy \\ &\geq \tau_2 \widehat{G}_t \int_{\Omega} (g_t(y) - G_t) \pi(y) dy \\ &= \tau_2 \widehat{G}_t (1 - G_t), \end{aligned} \quad (25)$$

where the inequality is obtained by applying $\Delta g_t(x_t) \geq 0, \bar{g}_t = \int g_t \rho_t \geq G_t$ and $\hat{g}_t(\cdot) \geq \widehat{G}_t, g_t(\cdot) \geq G_t$ in the last term. Therefore G_t can be lower bounded as

$$G_t \geq 1 - (1 - G_{t_0}) e^{\int_{t_0}^t -\tau_2 \widehat{G}_s ds}$$

In both Theorem 1 and Corollary 1, we assume (16) holds for any $t \geq t_0$, so

$$G_t \geq 1 - (1 - G_{t_0})e^{-\tau_2 c(t-t_0)} \quad (26)$$

Take it into (24), we get our final result: for any fixed t_0 ,

$$D_t + 1 - \frac{1}{Z_t} \leq (D_{t_0} + 1 - \frac{1}{Z_{t_0}}) \exp\{-\kappa_1(t - t_0) - \kappa_2 e^{-\tau_2 c(t-t_0)} + \kappa_2\}, \forall t \geq t_0 \quad (27)$$

The constants are defined as $\kappa_1 = 2\tau_1 + 2c\tau_2, \kappa_2 = \frac{2\tau_1(1-G_{t_0})}{\tau_2 c}$.

□

Remark 1.3. The estimate (26) shows that: starting from $G_0 \in [0, 1)$, G_t will strictly increase and converge to 1, as long as we have a lower bound for \widehat{G}_t . This is the reason why we do not need an assumption on existence of a lower bound for G_0 . The intuition is that, introducing exploration component allows us to loose the assumption on ρ_t .

Remark 1.4. In our result, we let $\tau_1, \tau_2 > 0$. It is slightly different from our implementation that $\tau_2 = 0$ when no new modes is found. However, this is not a big deal. If $\tau_2 = 0$ in dynamic (11), we can directly skip (23) in analysis and get a variation of (17):

$$D_t + 1 - \frac{1}{Z_t} \leq \left(D_{t_0} + 1 - \frac{1}{Z_{t_0}}\right) \exp\{-2\tau_1(t - t_0)\}, \forall t \geq t_0 \geq 0$$

Remark 1.5. From Theorem 1, we see the close relation between $1 - 1/Z_t$ and D_t . The limitation is that we do not have access to the explicit formula of Z_t . We speculate that it depends on the ratio between step size and skewness of π . Alternatively, we estimate Z_t in a specific numerical experiment (see figure 2), hoping to provide intuition on the relationship between exploration and convergence.

3.3 Further discussion

To make our theoretical analysis complete, we need to show that the assumption (16) is reasonable, that is, $\hat{\rho}/\pi$ can be lower bounded by a positive value, which highly depends on the quality of the Gaussian approximation.

Let us start from the uni-modal case: assume $\pi(x) \sim \exp(-V(x))$ has bounded support inside $\mathbf{B}_2(\mu, R)$, where μ is its unique mode. Let $\Sigma = -[\nabla^2 \log(\pi(\mu))]^{-1}$, we use $\hat{\rho}(x) := \mathcal{N}(\mu, \Sigma)$ to approximate π . We intend to give a lower bound for

$$\frac{\hat{\rho}(x)}{\pi(x)} = \frac{Z_\pi}{|\Sigma|^{1/2}(2\pi)^{d/2}} \exp\left(V(x) - \frac{(x - \mu)^T \Sigma^{-1} (x - \mu)}{2}\right)$$

Log-concavity and log-smooth implies that

$$\frac{M}{2} \|x - y\|_2^2 \leq V(y) - V(x) - \nabla V(x)^T (y - x) \leq \frac{L}{2} \|x - y\|_2^2$$

Without loss of generality we can assume $\mu = 0$ and $V(\mu) = 0$. Now we have

$$\frac{M}{2} \|x - \mu\|_2^2 \leq V(x) \leq \frac{L}{2} \|x - \mu\|_2^2$$

First, from $\Sigma^{-1} = \nabla^2 V(\mu)$, we have

$$M\mathbf{I}_d \preceq \Sigma^{-1} \preceq L\mathbf{I}_d \implies |\Sigma|^{\frac{1}{2}} \leq M^{\frac{d}{2}}$$

Then, we lower bound the normalizing constant of π :

$$Z_\pi = \int_{\mathcal{B}_2(\mu, R)} \exp(-V(x)) dx = \int_{\mathcal{B}_2(R)} \exp\left(-\frac{L}{2}\|x\|_2^2\right) dx$$

For normal vector $X \in \mathbb{R}^d$ with zero mean and covariance $\Sigma = L^{-1}\mathbf{I}_d$, we have $\mathbb{E}\|X\|_2 \leq \sqrt{d/L}$. We can use Gaussian concentration inequality to obtain a tail bound:

$$\begin{aligned} \Pr[\|X\|_2 \geq \mathbb{E}\|X\|_2 + t] &\leq \exp\left(-\frac{Lt^2}{2}\right), \forall t \geq 0 \\ \implies \Pr[\|X\|_2 \geq \sqrt{d/L} + t] &\leq \exp\left(-\frac{Lt^2}{2}\right), \forall t \geq 0 \end{aligned}$$

Let $R = \sqrt{d/L} + t$, then

$$\begin{aligned} Z_\pi &= \frac{(2\pi)^{d/2}}{L^{d/2}} (1 - \Pr[\|X\|_2 \geq R]) \\ &\geq \frac{(2\pi)^{d/2}}{L^{d/2}} \left[1 - \exp\left(-\frac{L}{2}(R - \sqrt{d/L})^2\right)\right], \forall R \geq \sqrt{d/L} \end{aligned} \quad (28)$$

Finally, in the uni-modal case, we can lower bound the fraction by

$$\begin{aligned} \frac{\hat{\rho}(x)}{\pi(x)} &= \frac{Z_\pi}{|\Sigma|^{1/2}(2\pi)^{d/2}} \exp\left(V(x) - \frac{(x - \mu)^T \Sigma^{-1}(x - \mu)}{2}\right) \\ &\geq \left(\frac{M}{L}\right)^{d/2} \left[1 - \exp\left(-\frac{L}{2}(R - \sqrt{d/L})^2\right)\right] \exp\left(-\frac{(L - M)R^2}{2}\right) \end{aligned} \quad (29)$$

We can easily extend this result to multimodal case with some mild assumptions. Suppose π has M modes and can be expressed by

$$\pi(x) = \sum_{i=1}^M w_i \pi_i(x), \text{ with } \sum_{i=1}^M w_i = 1, \text{ supp}(\pi) \subseteq \mathbf{B}_2(0, \frac{R}{2}) \quad (30)$$

where $\pi_i = \exp(-V_i(x))/Z_i$ is probability defined on $\mathbf{B}_2(\mu_i, R)$ with unique mode μ_i . We use the Gaussian mixture $\hat{\rho}(x)$ defined in (2) to approximate π . Notice that the support of π is contained in union of support of each π_i ,

$$\frac{\hat{\rho}(x)}{\pi(x)} = \frac{\sum_{i=1}^M \hat{w}_i \mathcal{N}(x; \mu_i, \Sigma_i)}{\sum_{i=1}^M w_i \pi_i(x)} \geq \min_{i \in [M]} \left\{ \frac{\hat{w}_i \mathcal{N}(x; \mu_i, \Sigma_i)}{w_i \pi_i(x)} \right\} \quad (31)$$

It is sufficient to give a lower bound for each component on the right hand side. Firstly, assume that each π_i is M_i -convex and L_i -smoothly, then we can give a bound for Z_i as in (28). Secondly, assume that the modes are well-separated, that is, $\pi(\mu_i) \approx w_i \pi_i(\mu_i)$. Then, recall the definition of estimated weights (1),

$$\hat{w}_i = \frac{w_i |\Sigma_i|^{1/2} Z_i^{-1}}{\sum_{j=1}^M w_j |\Sigma_j|^{1/2} Z_j^{-1}}$$

The denominator

$$\sum_{j=1}^M w_j \frac{|\Sigma_j|^{1/2}}{Z_j} \leq \sum_{j=1}^M w_j \cdot \max_{j \in [M]} \frac{|\Sigma_j|^{1/2}}{Z_j} \leq \max_{j \in [M]} \left(\frac{\kappa_j}{2\pi}\right)^{d/2} [1 - \Phi(R; L_j)]^{-1}$$

where $\kappa_j = L_j/M_j$ is condition number for the j^{th} mode, and $\Phi(R; L_j)$ is the probability of the norm of a zero-mean normal vector with covariance $L_j \mathbf{I}_d$ larger than $R - \sqrt{d/L_j}$. Therefore

$$\begin{aligned} \frac{\widehat{w}_i \mathcal{N}(x; \mu_i, \Sigma_i)}{w_i \pi_i(x)} &= \frac{1}{(2\pi)^{d/2} \sum_{j=1}^M w_j |\Sigma_j|^{1/2} Z_j^{-1}} \exp\left(V_i(x) - \frac{(x - \mu)^T \Sigma_i^{-1} (x - \mu)}{2}\right) \\ &\geq \min_{j \in [M]} \{\kappa_j^{-d/2} [1 - \Phi(R; L_j)]\} \cdot \exp(-(L_i - M_i)R^2/2) \end{aligned}$$

By applying (1), we obtain a theoretical result concerning Gaussian approximation to multimodal distribution:

Theorem 2. *The target distribution π is defined in (30), and the approximation distribution $\hat{\rho}$ is defined in (2). Suppose V_i is M_i -strongly convex and L_i -smoothly, then*

$$\inf_{\Omega} \frac{\hat{\rho}(x)}{\pi(x)} \geq \min_{j \in [M]} \left\{ \left(\frac{M_j}{L_j} \right)^{d/2} [1 - \Phi(R; L_j)] \right\} \cdot \min_{i \in [M]} \exp(-(L_i - M_i)R^2/2) \quad (32)$$

holds, where $\Phi(R; L_j)$ can be upper bounded by $\exp(-L_j(R - \sqrt{d/L_j})^2/2)$.

Theorem 2 draws a picture about how good or bad the Gaussian approximation can be, under some mild assumptions that takes multimodality into account. It gives a positive lower bound for \widehat{G}_t , under the condition that all modes have been discovered in the tempered level by time t . If we let $M = 1$, we directly get:

Corollary 2. *Target distribution $\pi \sim \exp(-V)$, with unique mode μ , is defined on $\Omega \subseteq \mathbb{B}_2(\mu, R)$. If V is M -strongly convex and L -smoothly, then (29) holds for any $x \in \Omega$.*

Remark 2.1. Denote the right hand side of (29) as a function $C(d, M, L, R)$. It decreases when the condition number $\kappa = L/M$ increases or the dimension d increases. It is under the curse of dimension. Still, it is sharp, because we can construct a function $V(x)$ that has Hessian $\nabla^2 V(\mu) = M \mathbf{I}_d$ locally, while $V(x) = L \|x - \mu\|_2^2/2$ for all $x \notin \mathbf{B}(\mu, \epsilon)$ for a ϵ arbitrarily small.

Remark 2.2. It is worth noticing that, $\exp(-(L - M)R^2/2)$ goes to 0 as $R \rightarrow \infty$. This implies, if π is unbounded, the lower bound c of \widehat{G}_t would be arbitrarily small unless our approximation match the tail behavior of the target distribution. This seems concerning, because matching the tail behavior of a non-trivial distribution by Gaussian approximation is almost impossible. However, in practice, we do need to be too concerned. The bound c is only used in (20) and (25), where the integral on low-probability regions does not matter too much. So we restrict ourselves to the case when π is a combination of bounded π_i (30), and one should not be worried about matching the tail behavior.

4 Numerical experiments

In numerical experiments, we compare the efficiency of our algorithm with BDLS and ALPS by using the same settings as in their original experiments. In order to highlight the importance of birth-death process, we also construct a degraded sampling scheme LEC by simply skipping the birth-death process in BDEC.

In BDEC algorithm, we keep N Markov chains instead of recording the trajectory of a single Markov chain as [15] did. These chains are independent while doing within-temperature updates, and they interact during birth-death process. So in order to compare fairly, the ALPS algorithm

we use is slightly different from its original version. We construct N independent Markov chains at each temperature level, update them according to the ALPS scheme and we do not record their trajectory. One iteration in ALPS contains $T - 1$ within-temperature updates and 1 swap move, which corresponds to T within-temperature updates in BDEC. We choose the Gaussian kernel $K(x, y) = \frac{1}{(2\pi h^2)^{d/2}} \exp(-|x - y|^2/2h^2)$. In our examples, we always choose $h = 0.05$, but it needs some tuning in other settings.

All experiments are conducted using Python 3.8.5 on a personal laptop with a 2 GHz Quad-Core Intel Core i5 processor. In each example, we run the algorithms for 10 times and average the results.

4.1 Example 1: 2D Gaussian mixture

In order to compare BDEC with the BDLS algorithm, we experiment on a 2-dimensional model from [16]. The target distribution is a mixture of four well-separated and heterogeneous 2-dimensional Gaussian distributions:

$$\pi(\mathbf{x}) = \sum_{i=1}^4 w_i \mathcal{N}(\mathbf{x}; \mu_i, \Sigma_i)$$

We keep 2000 samplers and they are initialized from the Gaussian distribution: $\mathcal{N}(\mathbf{x}; \mu_0, \Sigma_0)$. The parameters are defined by

$$w_i = \frac{1}{4}, i = 1, \dots, 4, \mu_0 = \mu_1 = (0, 8)^T, \mu_2 = (0, 2)^T, \mu_3 = (-3, 5)^T, \mu_4 = (3, 5)^T$$

$$\Sigma_0 = \begin{pmatrix} 0.3 & 0 \\ 0 & 0.01 \end{pmatrix}, \Sigma_1 = \Sigma_2 = \begin{pmatrix} 1.2 & 0 \\ 0 & 0.01 \end{pmatrix}, \Sigma_3 = \Sigma_4 = \begin{pmatrix} 0.01 & 0 \\ 0 & 2 \end{pmatrix}$$

We set time step $\Delta t = 0.005$ and kernel width $h = 0.05$ for both sampling schemes. We choose number of total iterations $J = 50$ and number of within-temperature moves $T = 6$ for BDEC, which equals 300 updates in BDLS. We choose hotter temperature $\beta_{hot} = 0.05$ for Markov chain Y and a batch size $B = 12$ for the Exploration Component. We compare the numerical results of estimating $\mathbb{E}(f)$ for different f in figure 1. The figures show that EC does accelerate the BDLS.

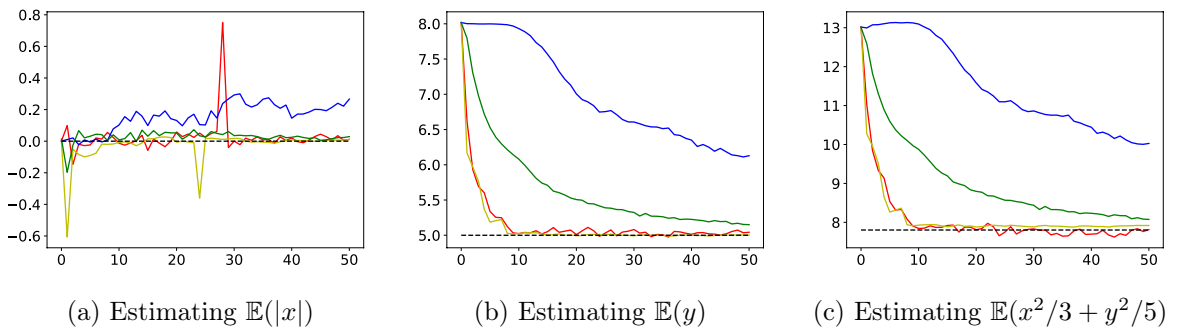


Figure 1: Results of estimating $\mathbb{E}(f)$ for three different f in Example 1. Red, estimation of BDEC; Yellow, LEC; Green, ALPS; Blue, BDLS; Black, the true expectation value. We plot the estimations for 50 total iterations with each iteration including 6 updates.

Z_t can be approximated by $\int_{\Omega_t} \pi(x) dx \approx \sum_{k=1}^K \mathbb{1}\{\omega_k \in \Omega_t\}$, if $\omega_k \stackrel{iid}{\sim} \pi$. As this example is a mixture of four equal-weighted Gaussian, we do have access to ω_k in advance. Based on (4),

we approximately let $\Omega_t = \bigcup_{i=1}^N \mathcal{B}(x_i^t, h)$. We set $K = 20000, h = 0.05$ and estimate Z_t in 50 steps (see figure 2a). As in Theorem 1, the χ^2 -divergence is bounded by $\frac{1}{Z_t} - 1$, we also plot the corresponding value $\frac{1}{Z_t} - 1$ in each step (see figure 2b).

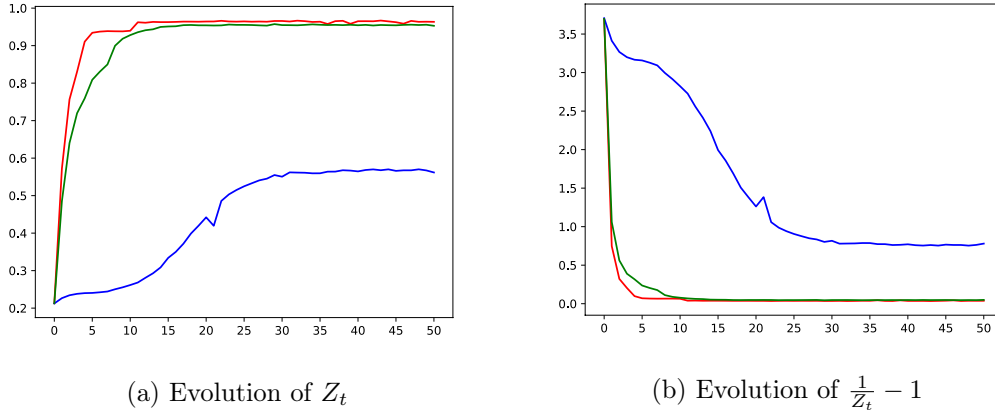


Figure 2: Red, BDEC; Green, ALPS; Blue, BDLS.

BDEC and ALPS have faster convergence speed than BDLS. This should be credited to the construction of a tempered level and the exploration component. Also notice that Z_t in BDEC process grows faster than in ALPS. This means, the information is efficiently passed to the target level by the MH step, so constructing annealed level is unnecessary. We will further discuss this point in another example 4.3.

4.2 Example 2: 2D Seemingly-Unrelated Regression Model

We also experiment on a 2-dimensional SUR model from [15] with parameters given in [35]. We omit the introduction of the background of the SUR model and give the target distribution directly:

$$\pi(\mathbf{x}) \propto e^{V(\mathbf{x})}, V(\mathbf{x}) = N \log(2\pi) + \frac{N}{2} \log(|\Sigma|) + N \quad (33)$$

after calculating the parameters given in [35], we can obtain the explicit formula:

$$\Sigma = \begin{pmatrix} 7.70x_1^2 - 19.27x_1 + 21.09 & 5.11x_1x_2 - 3.42x_1 - 3.51x_2 + 23.52 \\ 5.11x_1x_2 - 3.42x_1 - 3.51x_2 + 23.52 & 27.31x_2^2 - 97.40x_2 + 114.19 \end{pmatrix}$$

Our target distribution π has 2 modes: $\mu_1 = (0.78, 1.54)^T, \mu_2 = (2.76, 2.50)^T$. We keep 1000 samplers and they start from $\mu_0 = (1.25, 1.78)^T$ with a standard Gaussian noise.

Still, we set time step $\Delta t = 0.005$ and kernel width $h = 0.05$. Here, we choose number of total iterations $J = 30$ and number of within-temperature moves $T = 5$ for BDEC, which equals 30 total iterations and 4 within-temperature moves for ALPS (because the swap should be counted as one update). We choose hotter temperature $\beta_{hot} = 0.05$ for both algorithms and a batch size $\underline{B} = 12$ for the Exploration Component. We run ALPS using the same annealing scheme $(1, \sqrt{10}, 10)$ from [15]. We compare the absolute error of estimating $\mathbb{E}(f)$ for different f in Figure 3. Our results are consistent with the results in [15] that the ALPS algorithm has a rather large burn-in phase.

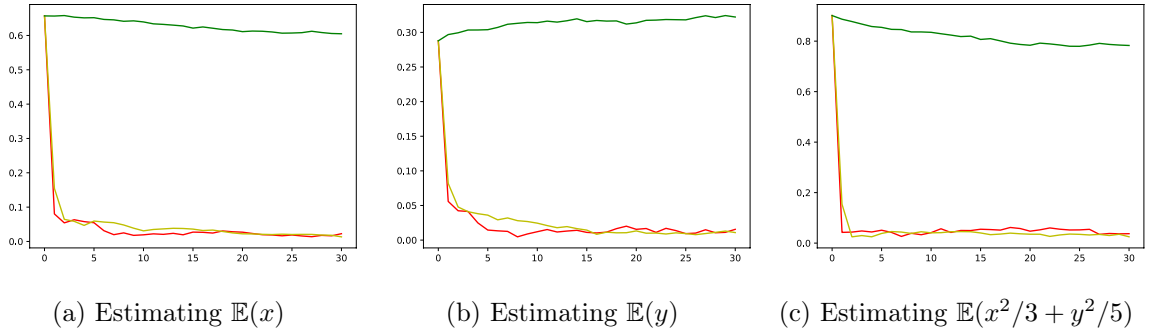


Figure 3: Errors of estimating $\mathbb{E}(f)$ for three different f in Example 2. Red, estimation of BDEC; Yellow, LEC; Green, ALPS; Blue, the true expectation value. We plot the estimations for 30 total iterations with each iteration including 5 updates.

4.3 Example 3: 20D Problem

For the last experiment, we run the algorithm in higher dimensions. The target distribution is a mixture of four well-separated 20-dimensional distributions with heterogeneous scaling used in [15]. The target distribution is given by

$$\pi(x) \propto \sum_{k=1}^4 \prod_{j=1}^{20} \frac{2}{w_k} \phi\left(\frac{x_j - (\mu_k)_j}{w_k}\right) \Phi\left(\alpha \frac{x_j - (\mu_k)_j}{w_k}\right) \quad (34)$$

where $\alpha = 10$, $\mu_1 = (20, 20, \dots, 20) = -\mu_2$, $\mu_3 = (-10, -10, \dots, -10, 10, 10, \dots, 10) = -\mu_4$, $w_1 = w_2 = 1$, $w_3 = w_4 = 2$, and $\phi(\cdot)$, $\Phi(\cdot)$ denote the density and CDF of standard Gaussian distribution.

We keep 1000 samplers and they are initialized from the first mode μ_1 with a standard Gaussian noise. We set time step $\Delta t = 0.001$ and a kernel bandwidth $h = 0.05$. We choose number of total iterations $J = 30$ and number of within-temperature moves $T = 3$ in each iteration for BDEC, which equals 30 total iterations and 2 within-temperature moves each iteration for ALPS. As suggested in [15], we set the inverse temperature $\beta_{hot} = 0.00005$ for both algorithms and an annealing scheme 1, 4, 16, 64, 256 for ALPS. For each iteration, we calculate KL-divergence of the first coordinate $KL(\rho_t^1 | \pi^1)$, where ρ_t^1, π^1 denotes the marginal distribution of ρ_t, π and $\rho_t = \sum_{i=1}^N \mathcal{N}(\cdot; x_i^t, h\mathbf{I})$ is the kernel distribution of N samplers. Because the marginal distributions of all coordinates are heterogeneous, the KL-divergence $KL(\rho_t^1 | \pi^1)$ can efficaciously show the convergence (see Figure 4).

To show the efficiency of BDEC, we compare the time one iteration takes in BDEC and in ALPS. The cpu time of one iteration in BDEC is about 936.79 and the birth-death process takes 6.81%, while the cpu time of one iteration in ALPS is about 1290.29, which is 37.74% higher than our algorithm. Therefore, it is established that BDEC has higher efficiency.

Noticeably, the result also tells us that the annealing part of ALPS is somehow useless. In ALPS, the annealing part helps overcome the problem of skewness: the annealed version of a skew target distribution is better approximated by mixture of Gaussian distribution, which means the acceptance rate of random walk Metropolis-Hastings is higher in colder temperature, thus the information of new modes can be more easily passed to the Markov chains. However, the cost is that multiple levels of Markov chains have to be kept simultaneously, which can be too time-consuming. In comparison, in BDEC scheme, the acceptance rate might be small due

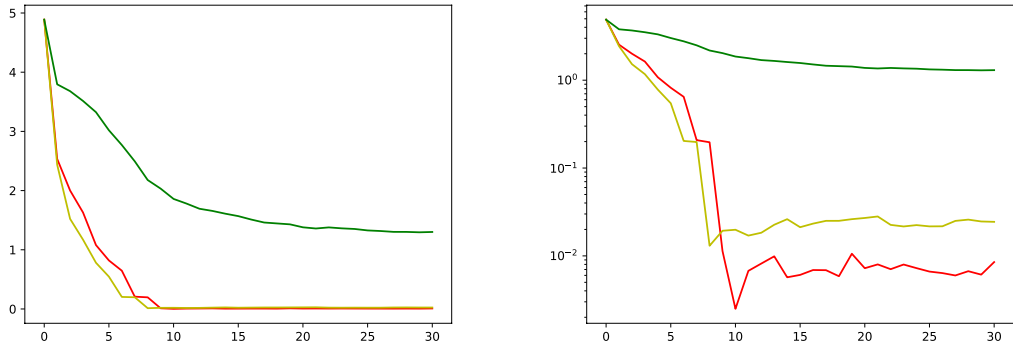


Figure 4: Convergence of KL-divergence of the 1st coordinate. Red, estimation of BLEC; Yellow, LEC; Green, BDLS. We plot the divergence for 30 total iterations with each iteration including 3 updates.

to skewness. But once a samplers reach the region around a new mode, the birth-death process will help transport a number of samplers to the new region instantly. So we get rid of the problem of skewness without multiplied cost. In general, BDEC is an effective scheme toward both multimodal and skewness.

5 Limitations and Further Work

Our results demonstrate that BDEC has outstanding performance, combining the advantages of both BDLS and ALPS. However, there are limitations and space for further discussion:

- Applications on practical settings: the experiment settings we use are artificial and have few numbers of modes. Distributions in real-world problems may have higher dimensions, larger scale, and more modes.
- Computational cost: we use exploration component to decide whether a mode is new and Gaussian approximation to propose locations around new modes. Both of them requires information about the second-order derivatives (see Eq.16 and Eq.5), which lead to high computational costs.
- Notice that the exponential convergence rate in Theorem 1 and Corollary 1 is $\kappa_1 = 2\tau_1 + 2c\tau_2$. This highlights the effort of BD and EC, but ignores the contribution of Langevin sampling. There might be sharper analysis that takes ULA into consideration.

Meanwhile, we notice that the convergence speed be astounding fast if $\tau_1, \tau_2 \rightarrow \infty$. However, in practice, there is no specific algorithm corresponds to this limiting situation. There is hope for deriving new sampling methods.

If we omit the technical details, the idea we present is simply *look before you leap*. ‘Look’ refers to letting Y explore the unknown space and collect useful information as much as possible. ‘Leap’ refers to X sampling the target distribution after having abundant information. Under this framework, we are actually proposing a toolbox for sampling multimodal distributions. It is free to substitute the Langevin Dynamics by other well-known Markov Chain Monte Carlo approaches. We can replace the Metropolis-Hastings step for the first few steps by directly

inserting new modes for the sake of simplicity. Also, we can apply the exploration component for multiple times instead of just one before X starts to move. In all, we are looking for variations of BDEC and their applications on wider range of problems.

References

- [1] Andrew Gelman, Walter R Gilks, and Gareth O Roberts. Weak convergence and optimal scaling of random walk metropolis algorithms. *The annals of applied probability*, 7(1):110–120, 1997.
- [2] Gareth O Roberts and Jeffrey S Rosenthal. Optimal scaling for various metropolis-hastings algorithms. *Statistical science*, 16(4):351–367, 2001.
- [3] Gareth O Roberts and Richard L Tweedie. Exponential convergence of langevin distributions and their discrete approximations. *Bernoulli*, pages 341–363, 1996.
- [4] Gareth O Roberts and Jeffrey S Rosenthal. Optimal scaling of discrete approximations to langevin diffusions. *Journal of the Royal Statistical Society: Series B (Statistical Methodology)*, 60(1):255–268, 1998.
- [5] Gareth O Roberts and Osnat Stramer. Langevin diffusions and metropolis-hastings algorithms. *Methodology and computing in applied probability*, 4:337–357, 2002.
- [6] Alain Durmus and Éric Moulines. High-dimensional Bayesian inference via the unadjusted Langevin algorithm. *Bernoulli*, 25(4A):2854 – 2882, 2019.
- [7] Alexandros Beskos, Natesh Pillai, Gareth Roberts, Jesus-Maria Sanz-Serna, and Andrew Stuart. Optimal tuning of the hybrid Monte Carlo algorithm. *Bernoulli*, 19(5A):1501 – 1534, 2013.
- [8] Tianqi Chen, Emily Fox, and Carlos Guestrin. Stochastic gradient hamiltonian monte carlo. In *International conference on machine learning*, pages 1683–1691. PMLR, 2014.
- [9] Raaz Dwivedi, Yuansi Chen, Martin J Wainwright, and Bin Yu. Log-concave sampling: Metropolis-hastings algorithms are fast! In *Conference on learning theory*, pages 793–797. PMLR, 2018.
- [10] Alain Durmus and Éric Moulines. On the geometric convergence for mala under verifiable conditions. *arXiv preprint arXiv:2201.01951*, 2022.
- [11] Keru Wu, Scott Schmidler, and Yuansi Chen. Minimax mixing time of the metropolis-adjusted langevin algorithm for log-concave sampling. *The Journal of Machine Learning Research*, 23(1):12348–12410, 2022.
- [12] Yin Tat Lee, Ruoqi Shen, and Kevin Tian. Structured logconcave sampling with a restricted gaussian oracle. In *Conference on Learning Theory*, pages 2993–3050. PMLR, 2021.
- [13] Xiang Cheng, Niladri S Chatterji, Peter L Bartlett, and Michael I Jordan. Underdamped langevin mcmc: A non-asymptotic analysis. In *Conference on learning theory*, pages 300–323. PMLR, 2018.

- [14] Charles J. Geyer. Markov chain monte carlo maximum likelihood. In *Interface Foundation of North America*, 1991. Retrieved from the University of Minnesota Digital Conservancy.
- [15] Nicholas G Tawn, Matthew T Moores, and Gareth O Roberts. Annealed leap-point sampler for multimodal target distributions. *arXiv preprint arXiv:2112.12908*, 2021.
- [16] Yulong Lu, Jianfeng Lu, and James Nolen. Accelerating langevin sampling with birth-death. *arXiv preprint arXiv:1905.09863*, 2019.
- [17] Yulong Lu, Dejan Slepčev, and Lihan Wang. Birth-death dynamics for sampling: Global convergence, approximations and their asymptotics. *arXiv preprint arXiv:2211.00450*, 2022.
- [18] Grant Rotskoff, Samy Jelassi, Joan Bruna, and Eric Vanden-Eijnden. Neuron birth-death dynamics accelerates gradient descent and converges asymptotically. In *International Conference on Machine Learning*, pages 5508–5517. PMLR, 2019.
- [19] Jonathan Goodman and Jonathan Weare. Ensemble samplers with affine invariance. *Communications in applied mathematics and computational science*, 5(1):65–80, 2010.
- [20] Michael Lindsey, Jonathan Weare, and Anna Zhang. Ensemble markov chain monte carlo with teleporting walkers. *SIAM/ASA Journal on Uncertainty Quantification*, 10(3):860–885, 2022.
- [21] Qiang Liu. Stein variational gradient descent as gradient flow. *Advances in neural information processing systems*, 30, 2017.
- [22] Sinho Chewi, Thibaut Le Gouic, Chen Lu, Tyler Maunu, and Philippe Rigollet. Sgvd as a kernelized wasserstein gradient flow of the chi-squared divergence. *Advances in Neural Information Processing Systems*, 33:2098–2109, 2020.
- [23] Enzo Marinari and Giorgio Parisi. Simulated tempering: a new monte carlo scheme. *Europhysics letters*, 19(6):451, 1992.
- [24] Nicholas G Tawn and Gareth O Roberts. Optimal temperature spacing for regionally weight-preserving tempering. *arXiv preprint arXiv:1810.05845*, 2018.
- [25] Nicholas G Tawn and Gareth O Roberts. Accelerating parallel tempering: quantile tempering algorithm (quanta). *Advances in Applied Probability*, 51(3):802–834, 2019.
- [26] Nicholas G Tawn, Gareth O Roberts, and Jeffrey S Rosenthal. Weight-preserving simulated tempering. *Statistics and Computing*, 30(1):27–41, 2020.
- [27] Jianfeng Lu and Eric Vanden-Eijnden. Methodological and computational aspects of parallel tempering methods in the infinite swapping limit. *Journal of Statistical Physics*, 174:715–733, 2019.
- [28] W. K. Hastings. Monte carlo sampling methods using markov chains and their applications. *Biometrika*, 57(1):97–109, 1970.
- [29] Manfred Opper and Cédric Archambeau. The variational gaussian approximation revisited. *Neural computation*, 21(3):786–792, 2009.
- [30] Matias Quiroz, David J Nott, and Robert Kohn. Gaussian variational approximations for high-dimensional state space models. *Bayesian Analysis*, 1(1):1–28, 2022.

- [31] Hakon Tjelmeland and Bjorn Kare Hegstad. Mode jumping proposals in mcmc. *Scandinavian journal of statistics*, 28(1):205–223, 2001.
- [32] Gareth O Roberts, Jeffrey S Rosenthal, and Nicholas G Tawn. Skew brownian motion and complexity of the alps algorithm. *Journal of Applied Probability*, 59(3):777–796, 2022.
- [33] Dimitris Bertsimas and John Tsitsiklis. Simulated annealing. *Statistical science*, 8(1):10–15, 1993.
- [34] Radford M Neal. Annealed importance sampling. *Statistics and computing*, 11:125–139, 2001.
- [35] Mathias Drton and Thomas S Richardson. Multimodality of the likelihood in the bivariate seemingly unrelated regressions model. *Biometrika*, 91(2):383–392, 2004.